EFFECT OF FINAL MACHINING ON CORROSION PROPERTIES AND STRESS CORROSION CRACKING SUSCEPTIBILITY OF AUSTENITIC STAINLESS STEEL

[1]Marek KUDLÁČ, [1]Mária DOMÁNKOVÁ, [1]Katarína BÁRTOVÁ, [1]Matúš GAVALEC, [1]Dávid SLNEK

[1]Slovak University of Technology in Bratislava, Faculty of Materials Science and Technology in Trnava, Trnava, Slovakia EU, marek.kudlac@stuba.sk, maria.domankova@stuba.sk, katarina.bartova@stuba.sk, matus.gavalec@stuba.sk, david.slnek@stuba.sk

https://doi.org/10.37904/metal.2024.4889

Abstract

Influence of various parameters of final machining on stress corrosion cracking of austenitic stainless steel was investigated. Boiling magnesium chloride solution was used as a medium for exposure of samples to find out the susceptibility for corrosion cracking. Residual stresses, the roughness, hardness of the surface layers, feed and cutting speed were the main parameters which were noticed, and their effect was evaluated and compared. The density of cracks on the surface of the machined samples was obtained, as well as the depth of these cracks into the material, while their morphology was also monitored using SEM. Light microscopy was used to monitor the surface after machining (before the corrosion test). Subsequently, the hardness was measured. The machined surface was also analysed using electrochemical methods such as potentiodynamic measurements and electrochemical potentiokinetic reactivation tests for intercrystalline corrosion susceptibility.

Keywords: Austenitic stainless steel, stress corrosion cracking, machining, surface, corrosion

1. INTRODUCTION

In areas of industry and energy, where components are exposed to corrosive environments, the use of austenitic stainless steels is considered. Their beneficial anti-corrosive properties due to passive layer and their preserved mechanical properties even at higher temperatures make them a suitable choice. Despite the excellent corrosion properties, there are ways in which these materials can succumb to corrosion [1,2].

A frequent problem with austenitic stainless steels is stress corrosion cracking. The susceptibility of austenitic stainless steels to stress corrosion cracking is in the environment of concentrated hot chloride solutions or steam containing chlorides. Cracks often initiate on existing surface defects (grooves, sharp edges, etc.) where the oxide layer has been broken or in pits or places where intergranular corrosion has occurred. Rough traces can also occur due to machining. After machining, residual stresses in the subsurface layers also occur, which can lead to corrosion cracking even without external loading [3].

Cracking mechanisms for austenitic stainless steels can be either an active dissolution mechanism [4], a passivation layer damage mechanism [5] or hydrogen embrittlement [6]. Austenitic corrosion-stainless steels can undergo a phase transformation to strain-induced martensite due to applied stress or hydrogen accumulation, making the material susceptible to brittle fracture [6].

In various articles, susceptibility of final machined samples to corrosion cracking was determined. The samples were analysed either in a simulated environment of the primary circuit [7] or in a boiling $MgCl_2$ solution (according to ASTM G36 [8]), which serves as an aggressive environment capable of causing stress corrosion cracking in stainless steels.

A significant problem with austenitic stainless steels in general is also susceptibility to intergranular corrosion caused by grain boundary depletion caused by the formation of $Cr_{23}C_6$ carbides. They arise in cases of incorrect heat treatment or with higher carbon contents [1].

The scientific goal of this work is to determine the susceptibility of austenitic stainless steel 08Ch18N10T to stress corrosion cracking in boiling $MgCl_2$ solution. Tension induced by residual stresses on the surface after turning can significantly affect this property. Also, the aim of the work is to determine the sensitivity to intergranular corrosion using the DL-EPR test. The benefit of this work is to show how machining can affect the corrosion resistance of such steels, while these results also have an impact on practice, especially in the energy industry.

2. MATERIALS AND METHODS

The material of samples used in this work was austenitic stainless steel type of GOST 08CH18N10T (AISI 321) in the form of a rod. The chemical composition of the material of the samples and 08CH18N10T standard are shown in **Table 1**. Compared to 08Ch18N10T standard, the material contained a slightly higher amount of Si and S. It also contained 0.66 wt. % Cu.

Table 1 Chemical composition of material of samples and standard chemical composition of 08Ch18N10T

Type of steel/norm	C (wt%)	Si (wt%)	Mn (wt%)	Cu (wt%)	Cr (wt%)	Ni (wt%)	Ti (wt%)	S (wt%)	P (wt%)
Material of samples	0.064	0.83	1.44	0.66	17.5	9.89	0.47	0.025	0.026
08Ch18N10T GOST 5632-72	≤ 0.08	≤ 0.8	≤ 2.0	–	17.0–19.0	9.0–11.0	≥ 5·C ≤ 0.70	≤ 0.020	≤ 0.035

A DMG CTX alpha 500 lathe was used to produce the samples which had the shape of a cylinder with a diameter of 38 mm and a length of 17 mm. In the experiment, a single-sided replaceable cutting plate made of sintered carbide marked VCGT 160404 with a sharp cutting edge and a tip radius of 0.4 mm was used. Work was done at two cutting speeds (100 and 250 m min^{-1}) and three different tool feeds (0.12, 0.2 and 0.3 mm). Depth of cut was 0.8 mm. Surface roughness was measured with a Mitutoyo SJ 210 surface roughness gauge. Rollers were cut into quarter cylindrical samples (**Figure 1**) where individual quarters were used for different analysis. One set of samples were metallographically prepared and electrolytic etched in 10% oxalic acid to develop the microstructure. Surface deformation zone depths after turning were observed using light microscope and microhardness HV 0.1 of subsurface zones was measured by the microhardness tester. The results of individual measurements are shown in **Table 2**.

Figure 1 Cut samples into quarter cylindrical shape

2.1 ASTM G36

The susceptibility of second set of turning samples of austenitic stainless steel (shape of 1/4 roller) to stress corrosion cracking was analysed by ASTM G36 [9]. The apparatus of this test consisted of an Erlenmeyer flask with an Allihn cooler on the top. 600 g of $MgCl_2 \cdot 6\ H_2O$ and 15 ml of demineralized water (approx. 46 wt. %)

was inserted into the Erlenmeyer flask and this solution was heated to 155 °C. After reaching a temperature of 155 °C – the solution was boiled, samples were placed in this solution. Exposition time in solution was 96 hours. Then the samples were taken out and rinsed in demineralized water and dried. In this way, the samples were prepared for monitoring the areal density of cracks on the machined surface and for determining the length/depth of the cracks into the interior of the material.

2.2 Analysis of samples after ASTM G36

Documentation of the turned surfaces was performed on JEOL JSM-IT300 scanning electron microscope. The analyses focused on the area in the middle of the surface. Crack density was evaluated using the ImageJ program. Initially, the area of the image at 500x magnification was determined in μm^2 (converted to mm^2). Subsequently, by measuring the length with a free hand, all the surface cracks that the image captured were marked. These lengths were summed. In this way, 5 representative images were taken in the central area of the machined surface of the sample. The sum of the crack lengths was divided by the area of the image, while the value was converted to mm^{-1}. **Figure 2** on the left side explains how to measure crack density using ImageJ on sample 1.

The samples were cut transverse section through the central part for the evaluation of crack length CL and crack depth CD to material. Subsequently, they were ground, polished, unetched and cleaned in ethanol. The preparation of the samples was followed by observation of cross section using SEM. In the case of the crack depth, it was the distance from the surface of the sample to the deepest point into which the crack extends. For the length of the crack, it was the total length of the crack (that is, the sum of the main crack together with the side branches). The procedure is shown in (**Figure 2**) on the right side.

The first and last sample (unexposed quarters of samples) were analysed by X-ray diffraction tensometry by Sin2ψ technique using the χ method. The measurement was carried out in the transverse and longitudinal direction of machining. The evaluated crystallographic plane was (222).

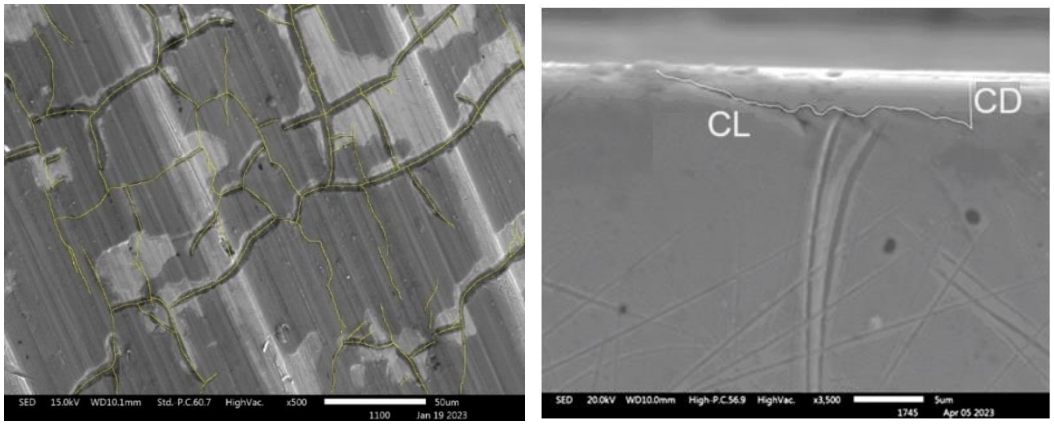

Figure 2 Crack density enhancement of sample 1 (left) and SEM image capturing the crack in sample 6 and marking both parameters: CL – crack length and CD – crack depth (right)

2.3 DL-EPR test

An electrochemical potentiokinetic reactivation test, double loop method (DL-EPR) was used to determine the degree of sensitization of given austenitic stainless steel to intergranular corrosion. This test uses a three-electrode connection in a flat corrosion cell. The use of this type of corrosion cell was necessary due to the round machined surfaces of the samples. The potentiostat used in work was GillAC by ACM Instruments. The working electrode was a turned surface of sample. The reference electrode was an Ag/AgCl electrode, and the auxiliary electrode was a platinum mesh. The DL-EPR test used a solution of 2 M H_2SO_4 and 0.05 M KSCN at a temperature of 30 °C. The use of a higher concentration of both components was due to the improvement

of the depassivation effect. Before the DL-EPR itself, open circuit potential was measured for 30 minutes. Subsequently, DL-EPR test was performed at a scanning speed of 1.67 mV/s.

3. RESULTS AND DISCUSSION

The machined surface and cross section of the samples was analysed using SEM. The density of cracks was determined from the images using the ImageJ program, as well as the depth and length of the cracks. Surface residual stresses were obtained by X-ray diffraction tensometry. The DL-EPR test followed these analyses.

3.1 Average crack density

From the images, the areal density of cracks was determined using the ImageJ program, which is shown in **Table 2**. It is obvious that the density of cracks has a certain repeating character. Crack density always increased with higher cutting speed v_c. On the contrary, it decreased with a lower cutting speed. In the case of sample 1 (53.8 ± 7.9 mm^{-1}), the smallest density of cracks is visible compared to the remaining samples. Sample 4 has the highest density of cracks (120.4 ± 14.1 mm^{-1}). The roughness of the samples increased with increasing feed while surface deformation zone depth does not show any significant dependence on other parameters. The determined residual stresses for sample 1 were 375 MPa in the longitudinal direction and 475 MPa in the transverse direction. As expected, sample 6 had higher residual stresses of 625 MPa in the longitudinal direction and 554 MPa in the transverse direction. It is visible that higher residual stresses also caused a higher density of cracks. The hardness decreased with increasing feed (sample 5 is an exception).

Table 2 Machining parameters and measured values of roughness, surface deformation zone depth, microhardness HV 0.1 and summary of crack density measurement results on the surface of samples 1 to 6

Sample	Tool feed f (mm)	Cutting speed v_c (m min^{-1})	Roughness R_a (µm)	Surface deformation zone depth (µm)	Microhardness HV 0.1 (-)	Average crack density (mm^{-1})
1	0.12	100	1.429	150	283 ± 14	53.8 ± 7.9
2	0.12	250	1.377	150	296 ± 16	90.0 ± 1.0
3	0.20	100	2.661	200	278 ± 26	71.2 ± 14.3
4	0.20	250	2.879	185	278 ± 18	104.2 ± 10.8
5	0.30	100	7.151	150	290 ± 15	72.5 ± 7.1
6	0.30	250	7.062	130	256 ± 11	120.4 ± 14.1

3.2 Crack depths and crack lengths

Lengths of cracks and depths of cracks were determined using ImageJ. These were then divided based on size into several size classes, shown in **Table 3**, while this is the percentage representation of all cracks in the given monitored area on the sample. In samples 1 and 2 they did not exceed 25 µm in length. In most cases, the representation of crack lengths was in the range from less than 5 to 25 µm, the same was the case with the depths. When evaluating the data, it was clear that the combination of the tool with positive geometry and the parameters – cutting speed v_c = 100 m min^{-1} and feed f = 0.12 mm will achieve a surface condition in which the resulting cracks will penetrate the interior of the material to the smallest extent compared to the other combinations of used turning parameters. As for the longest or the deepest cracks, so they were observed on sample 5, where there were cracks with lengths even between 55 and 60 µm. Also, samples 3, 4 and 6 had a representation of the length and depth of cracks greater than 30 µm. The analysis showed that in all cases the cracks propagated transgranularly.

Table 3 Percentage representation of crack lengths CL (upper values) and crack depths CD (values below in brackets) for individual samples (values of intervals are in μm; S. – Sample)

S.	CL (CD) < 5(%)	5≤CL (CD) < 10 (%)	10≤CL (CD) < 15 (%)	15≤CL (CD) < 20 (%)	20≤CL (CD) < 25 (%)	25≤CL (CD) < 30 (%)	30≤CL (CD) < 35 (%)	35≤CL (CD) < 40 (%)	40≤CL (CD) < 45 (%)	45≤CL (CD) < 50 (%)	50≤CL (CD) < 55 (%)	55≤CL (CD) < 60 (%)
1	9 (19)	39 (37)	35 (37)	12 (7)	5 (0)	0 (0)	0 (0)	0 (0)	0 (0)	0 (0)	0 (0)	0 (0)
2	4 (4)	36 (62)	45 (31)	11 (2)	4 (0)	0 (0)	0 (0)	0 (0)	0 (0)	0 (0)	0 (0)	0 (0)
3	8 (8)	16 (22)	13 (19)	22 (32)	24 (11)	11 (8)	3 (0)	0 (0)	0 (0)	3 (0)	0 (0)	0 (0)
4	13 (30)	44 (43)	21 (16)	6 (7)	9 (4)	6 (0)	0 (0)	0 (0)	1 (0)	0 (0)	0 (0)	0 (0)
5	11 (14)	23 (29)	22 (26)	14 (8)	8 (11)	10 (7)	4 (4)	3 (1)	0 (0)	4 (0)	0 (0)	1 (0)
6	8 (11)	16 (28)	13 (16)	19 (18)	16 (16)	18 (9)	6 (2)	2 (0)	2 (0)	0 (0)	0 (0)	0 (0)

3.3 DL-EPR test results

In (**Figure 3**) there is a scan of the DL-EPR curves of samples 1 to 6. The sensitization to intergranular corrosion can only be successfully determined on samples 1 and 2, since the increased roughness of the other samples was enormous to allow the reactivation maximum of the current density to be determined. Also, the similar roughness of samples 3 and 4 as well as samples 5 and 6 settled at a close current density in the passive state, but in the case of samples 5 and 6 it was an increase in the current density in the passive state by up to one order of magnitude. It is therefore obvious that despite the formation of the passivation layer, it does not fulfil its protective nature. The lowest values of the current density in the passive region were for samples 1 and 2, and for these samples the degree of sensitization was determined, which was at the level of 0.0005% (sample 1) and 0.0240% (sample 2). The EPR analysis of sample 1 was performed again and the value of the degree of sensitization was 0.0281%. Such a percentage of the degree of sensitization indicates that this material has not been sensitized (based on BS EN ISO 12732:2008 [10]). The measurement of sample 1 was more problematic, as the solution flowed and thus affected the shape of the curve (the reason for repeating the measurement).

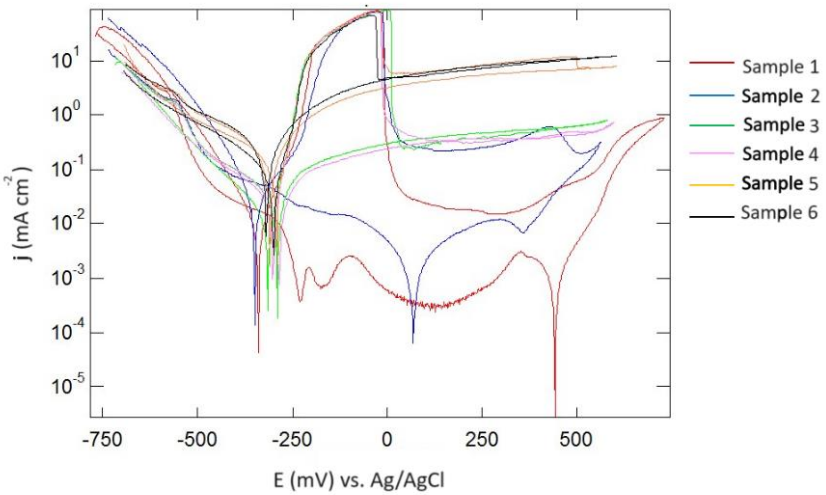

Figure 3 DL-EPR curves of all samples

4. CONCLUSION

A series of analyses and measurements were performed to monitor the effect of final turning on corrosion resistance and susceptibility to stress corrosion cracking of 08Ch18N10T samples:

- According to the ASTM G36 standard, experiments were carried out to determine the areal density of cracks and the depth or length of cracks. It turned out that the lowest density of cracks was in sample 1 – turned at a speed of 100 m min^{-1} and a feed of 0.12 mm (53.8 ± 7.9 mm^{-1}). The density of cracks increased at a speed of 250 m min^{-1} and with increasing feed (confirmed increase of residual stresses on the surface determined by X-ray diffraction tensometry). The lowest lengths and depths of cracks were again in sample 1 but also in sample 2. The length and depth of most of cracks in the samples ranged from 5 to 30 μm. The deepest and longest cracks were in sample 5, when the longest cracks were at the level between 55 and 60 μm (the length and depth increased at lower speed and higher feed). The nature of the cracks was transgranular.
- DL-EPR analysis revealed the degree of sensitization at the level of 0.0240% (0.0281%), so the samples 1 and 2 are taken as non-sensitized. As the roughness increased, the passivation current density increased, and this made it impossible to determine the degree of sensitization for samples 3 to 6.

In the near future, ASTM G36 tests will be performed on final turned AISI 316L and AISI 304 steel samples. Likewise, other types of final machining such as milling, grinding and others will be used. DL-EPR measurements at other concentrations will also be applied.

ACKNOWLEDGEMENTS

This work was supported by the Slovak Research and Development Agency under the Contract no. APVV-22-0146. This work was supported by the call for doctoral students and young researchers of Slovak University of Technology in Bratislava to start a research career (Grant 23-06-09-A).

REFERENCES

[1] PEDEFERRI, P. *Corrosion Science and Engineering*. Cham: Springer, 2018

[2] MCCAFFERTY, E. *Introduction to Corrosion Science*. Washington: Springer, 2010.

[3] LYNCH, S. Mechanistic and fractographic aspects of stress corrosion cracking. *Corrosion Reviews*. 2012, vol. 30, pp. 63-104.

[4] HOAR, T. P., WEST, J. M. Mechano-chemical anodic dissolution of austenitic stainless steel in hot chloride solution. *Proceedings of the Royal Society*. A268, 1962, pp. 304.

[5] NISHIMURA, R., MAEDA, Y. 2004. Stress corrosion cracking of type 304 austenitic stainless steel in sulphuric acid solution including sodium chloride and chromate. *Corrosion Science*. 2004, vol. 46, Issue 2, pp. 343-360.

[6] RHODES, P. R. Mechanism of Chloride Stress Corrosion Cracking of Austenitic Stainless Steels. *Corrosion.* 1969, vol. 25, Issue 11, pp. 462-472.

[7] ZHANG, W. et al. Combined effects of machining-induced residual stress and external load on SCC initiation and early propagation of 316 stainless steel in high temperature high pressure water. *Corrosion Science*, 2021, vol. 190, pp. 1-13.

[8] GOSH, S. et al. Role of residual stresses induced by industrial fabrication on stress corrosion cracking susceptibility of austenitic stainless steel. *Materials and Design*. 2011, vol. 32, pp. 3823-3831.

[9] ASTM G36-00: *Standard Practice for Evaluating Stress-Corrosion-Cracking Resistance of Metals and Alloys in a Boiling Magnesium Chloride Solution*. West Conshohocken, PA, USA: ASTM International, 2000.

[10] BS EN ISO 12732:2008. *Corrosion of metals and alloys. Electrochemical potentiokinetic reactivation measurement using double loop method (based on Cihal's method)*, United Kingdom: BSI, 2008.